To the Graduate Council:

I am submitting herewith a thesis written by Guy H. Lee entitled "Laminar Natural Convection Heat Transfer along a Needle with Thermal Radiation." I have examined the final copy of this thesis for form and content and recommend that it be accepted in partial fulfillment of the requirements for the degree of Master of Science, with a major in Engineering Science.

K H Kim

K. H. Kim, Major Professor

We have read this thesis and
recommend its acceptance:

Carl J. Remenyik

Osama Soliman

Accepted for the Council:

CW Minkel

Vice Provost
and Dean of The Graduate School

LAMINAR NATURAL CONVECTION HEAT TRANSFER ALONG A NEEDLE WITH THERMAL RADIATION

A Thesis

Presented for the

Master of Science

Degree

The University of Tennessee, Knoxville

Guy H. Lee

December 1987

ACKNOWLEDGMENTS

My deepest appreciation and thanks go to Dr. K. H. Kim, who acted as my advisor during both my undergraduate years and my graduate studies. He provided many helpful suggestions and encouragements which helped me to overcome many difficulties encountered in my study. He was always willing to provide me with direction during my stay at the University of Tennessee. Thanks also goes to Dr. C. J. Remenyik and Dr. M. O. Soliman who acted as my thesis committee members.

ABSTRACT

The purpose of this study was to investigate laminar natural convection heat transfer along a thin needle with radiative heat flux. In particular, the investigation centered on the skin friction factor and heat transfer rate as well as the velocity and temperature profiles along the transformed spatial variable η. The radiative heat flux term was linearized after being simplified by means of Rosseland approximation. The study was initiated by finding transformation variables which reduced the original boundary layer equations in cylindrical coordinate into ordinary differential equations. Through this transformation, a certain condition about the needle shape was found to guarantee such a transformation exists. Then the relationships between skin friction factor and transformed velocity function, as well as heat transfer rate and transformed temperature function, were formulated to establish the relationship between these transformed variables and real dimensional values.

These coupled ordinary differential equations were solved by one type of shooting method which took into account the fact that some boundary conditions were prescribed at infinity. This scheme guessed initial conditions such as the slope of velocity and temperature at the wall and examined the convergence of the boundary conditions at infinity by means of integration. This scheme was stable in a sense that any values of initial guesses are automatically corrected for convergence and the error term was well controlled within the tolerance bound.

The values of skin friction factor and heat transfer rate at the wall were calculated in terms of similarity variables for several values of Prandtl numbers and parameters of conduction to radiation ratio. Also several profiles for the momentum and thermal boundary layer were presented in graphs for different values of Prandtl numbers and parameters of conduction to radiation ratio. This information leads to the conclusion about the effect of

the degree of radiative influence as well as the role of Prandtl numbers. This study can provide valuable information about the heat transfer and skin friction along the slender wire especially in high temperature.

TABLE OF CONTENTS

CHAPTER PAGE

I. INTRODUCTION 1

II. MATHEMATICAL ANALYSIS OF THE NATURAL CONVECTION ALONG THE NEEDLE 4

Boundary Layer Equations for the Needle Shape. 6

Similarity Transformation for the Boundary Layer Equations . . . 13

Analysis of Similarity Equations 21

III. ANALYSIS OF THE SIMILARITY SOLUTION 26

General Feature of the Shooting Method 26

Satisfaction of Asymptotic Boundary Conditions 27

Result of the Solution Algorithm 31

IV. CONCLUSIONS AND RECOMMENDATIONS 46

LIST OF REFERENCES 48

VITA 51

LIST OF FIGURES

FIGURE	PAGE
1 Geometry of the Problem	5
2 Transformed skin friction $f''(\eta_o)$ vs. needle shape parameter η_o with no radiation	34
3 Transformed skin friction $f''(\eta_o)$ vs. needle shape parameter η_o N (conduction to radiation ratio) = 1.0	35
4 Transformed skin friction $f''(\eta_o)$ vs. needle shape parameter η_o N (conduction to radiation ratio) = 0.1	36
5 Transformed heat transfer rate $g'(\eta_o)$ vs. needle shape parameter η_o with no radiation	37
6 Transformed heat transfer rate $g'(\eta_o)$ vs. needle shape parameter η_o N (conduction to radiation ratio) = 1.0	38
7 Transformed heat transfer rate $g'(\eta_o)$ vs. needle shape parameter η_o N (conduction to radiation ratio) = 0.1	39
8 Similarity temperature profile with η_o = 0.001 and no radiation	40
9 Similarity velocity profile with η_o = 0.001 and no radiation	41

10 Similarity temperature profile
with η_o = 0.1 and no radiation 42

11 Similarity velocity profile
with η_o = 0.1 and no radiation 43

12 Similarity temperature profile
with η_o = 0.1 and Prandtl number = 10.0 44

13 Similarity velocity profile
with η_o = 0.1 and Prandtl number = 10.0 45

LIST OF SYMBOLS

τ	shear stress
$\mathbf{r}, \mathbf{z}$	spatial variables in real dimension
r'', z''	spatial variables in non-dimensional form
r, z	spatial variables in non-dimensional and scaled form
$\mathbf{u}_z, \mathbf{u}_r$	z and r velocity in real dimension
u''_z, u''_r	z and r velocity in non-dimensional form
u_z, u_r	z and r velocity in non-dimensional and scaled form
Ψ	stream function
T	temperature
c_p	specific heat
k	thermal conductivity
g	gravitational constant
μ	dynamic viscosity
ν	kinematic viscosity
α	thermal diffusivity
ρ	density
β	thermal expansion coefficient
P	pressure
L	characteristic length
w	reference velocity
q_r	radiative heat flux
σ	Stefan-Boltzman constant
λ	thermal radiation wave length
c	absortivity

$\tau_{o\lambda}$	optical thickness
τ_ρ	photon mean free path
N	conduction to radiation ratio ($=\frac{4\lambda^2\sigma T_\infty^{\ 3}}{kc_p}$)
Re	Reynolds number ($=\frac{Lw}{\nu}$)
Pr	Prandtl number ($=\frac{\nu}{\alpha}$)
Gr	Grashof number ($=\frac{g\beta(T_o - T_\infty)L^3}{\nu^2}$)
h	heat transfer coefficient
Nu	Nusselt number ($=\frac{hL}{k}$)
θ	dimensionless temperature
A	similarity transformation parameter
η	independent similarity variable
η_o	needle shape parameter
f	stream function in similarity transformation
g	similarity temperature function
f'	similarity velocity function
f''	transformed skin friction
g'	transformed heat transfer rate
E	error term

subscript $_o$ denotes the condition at the wall

$_\infty$ denotes the condition at the edge of the boundary layer

superscript $\overline{}$ denotes average value

CHAPTER I

INTRODUCTION

Over the last two decades, considerable attention has been devoted to predicting the flow and heat transfer for problems where the flow is two-dimensional (e.g., vertical plates and cylinders, tilted plates, horizontal circular cylinders) or axisymmetric (e.g., spheres). The literature contains many references to investigators by various researchers [1 - 4, 12]. Particular interest in this study is directed toward the prediction of skin friction and heat transfer rate at the wall as well as temperature and velocity profiles along the isothermal thin needle. In this study, the parabolic needle was assumed to represent a very small diameter cylinder compared to its length such as wires and sensors of hot wire. Therefore the curvature effect is neglected.

Several investigators published different aspects of the needle problem. T. Cebeci and Y. Na [2] solved an isothermal needle problem using the similarity technique. J. Narain [1] extended that result to include a constant heat flux at the wall. G. Raithby et al. [4] reported experimental results from a needle problem considering the curvature effect. J. Narain [3] solved that problem by the finite difference scheme utilizing the non-similarity concept. This study assumed that the needle remained at a constant temperature during the whole process.

The isothermal needle is assumed to be immersed in a large fluid reservoir which remains at a constant temperature. The temperature difference between the needle and the ambient fluid causes density variation of the fluid along the needle. The lack of balance between gravitational force and bouyance force due to density variation results in fluid movement and temperature variation along the needle. In this study, the friction factor and heat transfer rate along the needle, as well as the temperature and velocity profile along the fluid, were investigated.

Another aspect of this study was devoted to the influence of radiation, which implied the needle temperature is high enough to assure the influence of radiation. The effect of thermal radiation on heat transfer in the laminar boundary layer flow in an absorbing and emitting medium have been studied by several investigators. Viskanta and Grosh [7], and Kim et al. [8] solved numerically the problem of laminar flow over a wedge for the optically thick boundary layer by using a numerical technique and local similarity approach. Novotny and Yang, and Goulard [9 - 10] have considered the optically thick approximation for boundary layer flow over a flat plate. Kim and Ozisik [11] solved the heat transfer problem of an absorbing, emitting, isotropically scattering stagnation point boundary layer flow by treating the radiation part of the problem exactly with the normal-mode-expansion technique. In this study, the Rosseland approximation was employed to represent heat flux due to thermal radiation.

The needle problem of physical dimensions is transformed into a non-dimensional scaled form. Use of the free parameter technique described in [13] transformed non-dimensional equations into ordinary differential equations with a certain value for a transformation parameter. The resulting differential equations are solved by the shooting method.

The situation investigated here needs evaluation of boundary conditions at infinity. This difficulty was overcome by adapting the asymptotic satisfaction of boundary conditions. By predicting the missing initial values, the resulting set of equations became the initial value problem. Then checking the satisfaction of the boundary conditions at infinity will assure that the guess of initial values is correct. If boundary conditions are not satisfied by a certain initial guess, the scheme adjusts the initial guess to meet the criteria.

In the present investigation, the development of equations for the momentum and energy transport in the boundary layer along an isothermal slender needle are first discussed. In chapter II, the derivation of similarity transformation will be presented with the brief introduction of thermal radiation. In chapter III, the analysis of the similarity solution and the results are discussed in detail. The results include graphs depicting the similarity forms of the temperature and velocity distribution as well as the effect of needle shape upon the skin friction and heat transfer rate.

CHAPTER II

MATHEMATICAL ANALYSIS OF THE NATURAL CONVECTION ALONG THE NEEDLE

Unlike the forced convection heat transfer, natural convection heat transfer always gives coupled equations between momentum and energy equations. That accounts for the fact that the movement of fluid is due to the variation of densities which is caused by the temperature difference between each fluid layers.

This study concerns the temperature and velocity variations along the needle which is immersed in a large fluid field. The prime interest of this study is to investigate the effects of thermal radiation on the skin friction and heat transfer rate for the shape of a needle and the effect of various values of parameters of conduction to radiation ratio and Prandtl numbers on the velocity and temperature profiles.

With rare exceptions, compressibility effects in flows caused by natural convective heat transfer may be ignored. Here the flow will be assumed to be incompressible and laminar. Viscosity and thermal conductivity are approximated by constants.

The continuity, Naiver-Stokes, and energy equations in terms of cylindrical coordinates for the geometry in Fig. 1 are

$$\frac{\partial v_r}{\partial r} + \frac{1}{r} v_r + \frac{\partial v_z}{\partial z} = 0 , \tag{1.1}$$

$$\rho(v_r \frac{\partial v_r}{\partial r} + v_z \frac{\partial v_r}{\partial z}) = - \frac{\partial P}{\partial r} + \mu(\frac{\partial^2 v_r}{\partial r^2} + \frac{1}{r}\frac{\partial v_r}{\partial r} + \frac{\partial^2 v_r}{\partial r^2}) , \tag{1.2}$$

$$\rho(v_r \frac{\partial v_z}{\partial r} + v_z \frac{\partial v_z}{\partial z}) = - \frac{\partial P}{\partial z} + \mu(\frac{\partial^2 v_z}{\partial r^2} + \frac{1}{r}\frac{\partial v_z}{\partial r} + \frac{\partial^2 v_z}{\partial r^2}) - \rho g, \tag{1.3}$$

$$\rho c_p(v_r \frac{\partial T}{\partial r} + v_z \frac{\partial T}{\partial z}) = k(\frac{1}{r}\frac{\partial T}{\partial r} + \frac{\partial^2 T}{\partial r^2} + \frac{\partial^2 T}{\partial z^2}) - \frac{\partial q_r}{\partial r} - \frac{1}{r} q_r. \tag{1.4}$$

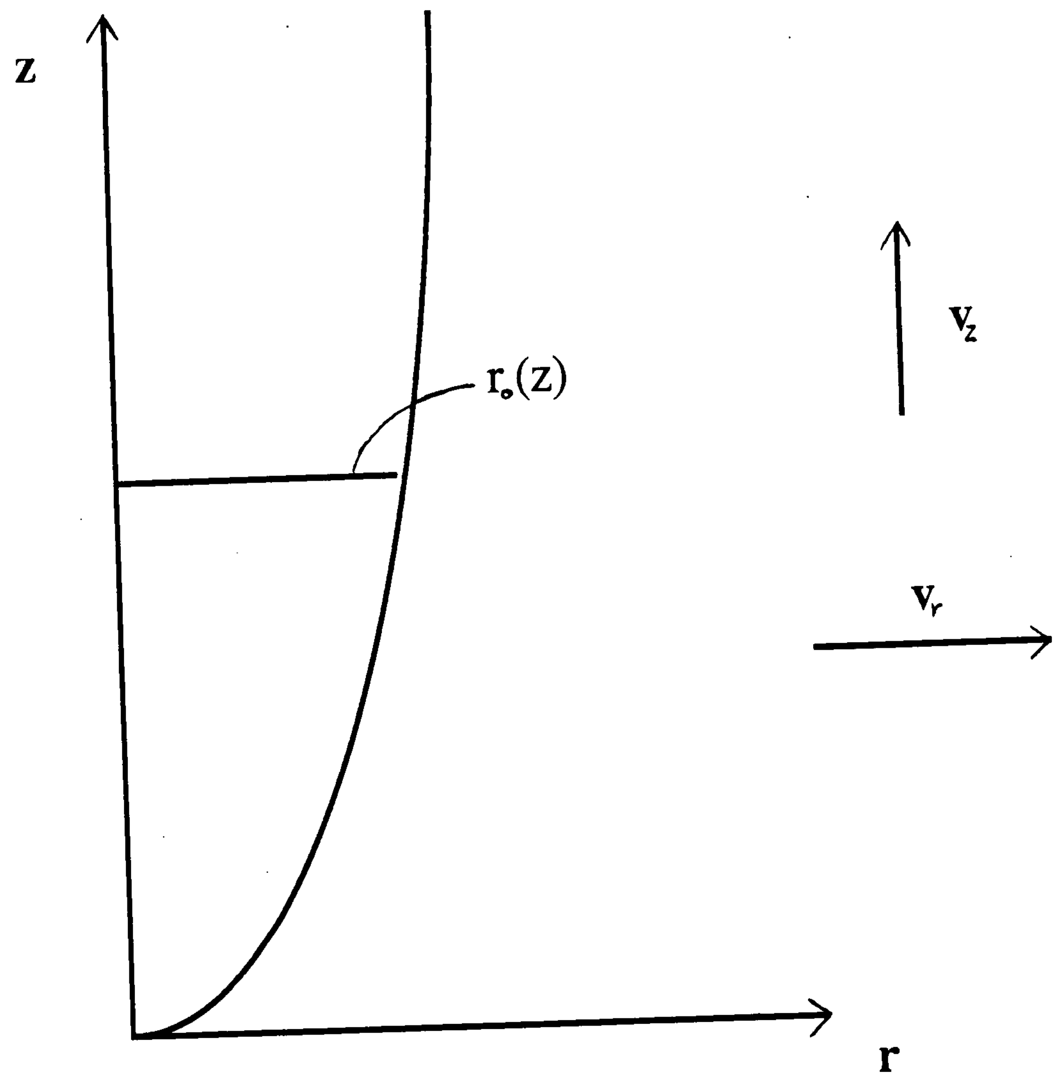

Fig. 1. Geometry of the problem

where

q_r = radiative heat flux.

The assumptions involved in this study are

1. Dissipation may be ignored. This assumption is valid in this case because of the high temperatures and the low velocities.
2. Radiational properties of the medium do not depend on the frequencies.
3. Radiational transport through the medium affects only molecules in close proximity.
4. Most fluid properties remain constant through the whole process.
5. Flow is assumed to be laminar.

2.1 BOUNDARY LAYER EQUATIONS FOR THE NEEDLE SHAPE

With the usual comparison test, the above equations (1.1) - (1.4) can be reduced to the usual boundary layer equations. If we assumed the radius of a needle cross-section is small everywhere compared to the length of the needle, the pressure term in equation (1.3) can be treated as a function of z only.

$$\frac{\partial P}{\partial z} = \frac{dP}{dz} = \frac{dP_\infty}{dz}$$

The momentum and energy equation for the boundary layer equations become

$$\rho\left(v_r \frac{\partial v_z}{\partial r} + v_z \frac{\partial v_z}{\partial z}\right) = -\frac{dP_\infty}{dz} + \mu\left(\frac{\partial^2 v_z}{\partial r^2} + \frac{1}{r}\frac{\partial v_z}{\partial r}\right) - \rho g, \qquad (2.1.1)$$

$$\rho c_p(v_r\frac{\partial T}{\partial r} + v_z\frac{\partial T}{\partial z}) = k(\frac{1}{r}\frac{\partial T}{\partial r} + \frac{\partial^2 T}{\partial r^2}) - \frac{q_r}{\partial r} - \frac{1}{r}q_r. \qquad (2.1.2)$$

First, the momentum equation will be derived through the expression for bouyance force.

Noting further that $\frac{dP_\infty}{dz}$ is the hydrostatic pressure gradient dictated by ρ_∞, $\frac{dP_\infty}{dz} = -g\rho_\infty$, the momentum equation (2.1.1) becomes

$$\rho(v_r\frac{\partial v_z}{\partial r} + v_z\frac{\partial v_z}{\partial z}) = \mu(\frac{\partial^2 v_z}{\partial r^2} + \frac{1}{r}\frac{\partial v_z}{\partial r}) - (\rho - \rho_\infty)\, g. \qquad (2.1.3)$$

After expanding ρ at ρ_∞ by Taylor series, ρ can be expressed as

$$\rho = \rho_\infty[1 - \beta(T - T_\infty)],$$

where

β = thermal expansion coefficient.

The above expression for ρ simplifies momentum equation (2.1.3) as

$$\rho(v_r\frac{\partial v_z}{\partial r} + v_z\frac{\partial v_z}{\partial z}) = \mu(\frac{\partial^2 v_z}{\partial r^2} + \frac{1}{r}\frac{\partial v_z}{\partial r}) + g\beta(T - T_\infty). \qquad (2.1.4)$$

The energy equation will be derived with the consideration of the radiative heat flux term. In case of radiating media, the degree of absorbing radiation of the medium has an effect on radiation transport by the medium. The measure of this capability is defined as the optical thickness of the medium. Consider a non-scattering medium, and let L be a characteristic length. In this study, the length of a needle was chosen to be a characteristic length. If the absorption coefficient c is independent of temperature, the monochromatic optical thickness of the medium is defined as

$$\tau_{o\lambda} = cL.$$

The photon mean free path, which is defined as the average distance travelled by a photon before it collides into other photons, may be expressed as

$$\tau_{\rho} = \frac{1}{c}.$$

Substituting the absorption coefficient in the monochromatic optical thickness with the photon mean free path gives an expression for the optical thickness as

$$\tau_{o\lambda} = \frac{L}{1/c} = \frac{L}{\tau_{\rho}}.$$

The above expression shows that $\tau_{o\lambda}$ is the ratio of the characteristic length to the photon mean free path.

In an optically thick assumption, radiation emitted from individual molecules affects only molecules in close proximity. In other words, the photon mean free path is much smaller than the characteristic length and one may think that medium is continuum with respect to radiation. In an optically thick assumption, the energy transport process becomes one of a diffusion type. Findings indicate that if consideration is confined to an optically thick medium, the so-called Rosseland approximation may be employed to represent the radiation heat flux q_r. This approximation is given by the expression

$$q_r = -\frac{4\lambda^2\sigma}{3c}\frac{\partial T^4}{\partial r},$$

where

c = absorption coefficient

σ = Stefan-Boltzman constant

λ = wave length of the emitted radiation.

The Rosseland approximation to the radiative heat flux term may be linearized by taking the Taylor expansion for T^4 around T_∞. Then q_r is expressed as

$$q_r = -\frac{16\lambda^2\sigma}{3c} T_\infty^{\,3}\frac{\partial T}{\partial r}.$$

Then the conduction heat transfer term and heat transfer term due to radiation can be combined as

$$\alpha(1 + \frac{4}{3N})\,(\frac{1}{r}\frac{\partial T}{\partial r} + \frac{\partial^2 T}{\partial r^2}),$$

where

$$N = \frac{4\lambda^2\sigma T_\infty^{\,3}}{kc_p},\ \text{conduction to radiation ratio.}$$

The above expression may simplify energy equation (2.1.2) as

$$v_r\frac{\partial T}{\partial r} + v_z\frac{\partial T}{\partial z} = \alpha(1 + \frac{4}{3N})\,(\frac{1}{r}\frac{\partial T}{\partial r} + \frac{\partial^2 T}{\partial r^2}). \qquad (2.1.5)$$

Equations (2.1.4) - (2.1.5) and the continuity equation are non-dimensionalized by the new variables defined as

$$r'' = \frac{r}{L}, \quad z'' = \frac{z}{L}, \quad v_r'' = \frac{v_r}{w}, \quad v_z'' = \frac{v_z}{w},$$

where

L = characteristic length

w = reference velocity.

The continuity equation becomes

$$\frac{\partial v''_r}{\partial r''} + \frac{1}{r''} v''_r + \frac{\partial v''_z}{\partial z''} = 0. \qquad (2.1.6)$$

The momentum equation becomes

$$L\rho\left(v''_r \frac{\partial v''_z}{\partial r''} + v''_z \frac{\partial v''_z}{\partial z''}\right) = \frac{\mu}{w}\left(\frac{\partial^2 v''_z}{\partial r''^2} + \frac{1}{r''}\frac{\partial v''_z}{\partial r''}\right) + \frac{L^2}{w^2} g\beta(T - T_\infty). \qquad (2.1.7)$$

The energy equation becomes

$$Lv''_r \frac{\partial T}{\partial r''} + Lv''_z \frac{\partial T}{\partial z''} = \frac{\alpha}{w}\left(1 + \frac{4}{3N}\right)\left(\frac{1}{r''}\frac{\partial T}{\partial r''} + \frac{\partial^2 T}{\partial r''^2}\right). \qquad (2.1.8)$$

Equations (2.1.6) - (2.1.8) are scaled in order to show the significant parameters involved in this study. Scaling transformation is performed through new variables defined as

$$r = (Re)^{1/2} r'' , \tag{2.1.9}$$

$$z = \frac{w^2}{\beta g(T_o - T_\infty)L} z'', \tag{2.1.10}$$

$$v_r = (Re)^{1/2} v_r'', \tag{2.1.11}$$

$$v_z = \frac{w^2}{\beta g(T_o - T_\infty)L} v_z'' . \tag{2.1.12}$$

The continuity equation becomes

$$\frac{\partial v_r}{\partial r} + \frac{1}{r} v_r + \frac{\partial v_z}{\partial z} = 0. \tag{2.1.13}$$

The momentum equation becomes

$$v_r \frac{\partial v_z}{\partial r} + v_z \frac{\partial v_z}{\partial z} = \frac{T - T_\infty}{T_o - T_\infty} + \frac{1}{r}\frac{\partial v_z}{\partial r} + \frac{\partial^2 v_z}{\partial r^2} . \tag{2.1.14}$$

The energy equation becomes

$$v_r \frac{\partial T}{\partial r} + v_z \frac{\partial T}{\partial z} = \frac{\alpha}{Lw} Re(1 + \frac{4}{3N})(\frac{1}{r}\frac{\partial T}{\partial r} + \frac{\partial^2 T}{\partial r^2}) \tag{2.1.15}$$

The $\frac{\alpha}{Lw}$ Re term in equation (2.1.15) can be simplified as $\frac{1}{Pr}$ and temperature can be non-dimensionalized by new variable θ defined as

$$\theta = \frac{T - T_\infty}{T_o - T_\infty} . \tag{2.1.16}$$

Then the energy equation becomes

$$v_r\frac{\partial\theta}{\partial r} + v_z\frac{\partial\theta}{\partial z} = \frac{1}{Pr}\left(1+\frac{4}{3N}\right)\left(\frac{1}{r}\frac{\partial\theta}{\partial r} + \frac{\partial^2\theta}{\partial r^2}\right). \tag{2.1.17}$$

The boundary conditions for this case are

at $r = r_o(z)$

$$v_r = 0 \tag{2.1.18}$$

$$v_z = 0 \tag{2.1.19}$$

$$\theta = 1 \tag{2.1.20}$$

for $r \rightarrow \infty$

$$v_z \rightarrow 0 \tag{2.1.21}$$

$$\theta \rightarrow 0. \tag{2.1.22}$$

2.2 SIMILARITY TRANSFORMATION FOR THE BOUNDARY LAYER EQUATIONS

This study uses a one parameter group transformation to derive similarity equations from the boundary layer equations. The procedures for obtaining similarity equations can be divided into four steps. The first step is to define a linear transformation group for independent variables and dependent variables. The second step is to determine the relationship between the constants involved in the transformation with the condition of invariancy. The third step is to eliminate the transformation parameter to determine absolute invariants under that transformation. The fourth step is to find a condition under which boundary conditions can be transformed. In the fourth step, it will be shown that a certain restriction is imposed upon the shape of the needle.

Equations (2.1.13), (2.1.14), and (2.1.17) can be simplified by introducing the stream function Ψ, which automatically satisfies the continuity equation. The stream function is defined as

$$v_r = -\frac{1}{r}\frac{\partial \Psi}{\partial z}\ , \ v_z = \frac{1}{r}\frac{\partial \Psi}{\partial r}\ . \tag{2.2.1}$$

The momentum equation is written in terms of stream function as

$$\frac{1}{r^2}\frac{\partial \Psi}{\partial z}\frac{\partial^2 \Psi}{\partial r^2} + \frac{1}{r^3}\frac{\partial \Psi}{\partial z}\frac{\partial \Psi}{\partial r} + \frac{1}{r^2}\frac{\partial \Psi}{\partial r}\frac{\partial^2 \Psi}{\partial z \partial r} = \frac{1}{r}\frac{\partial^3 \Psi}{\partial r^3} - \frac{1}{r^2}\frac{\partial^2 \Psi}{\partial r^2} + \frac{1}{r^3}\frac{\partial \Psi}{\partial r} - \theta. \tag{2.2.2}$$

The energy equation is written in terms of stream function as

$$-\frac{1}{r}\frac{\partial\Psi}{\partial z}\frac{\partial\theta}{\partial r}+\frac{1}{r}\frac{\partial\Psi}{\partial r}\frac{\partial\theta}{\partial z}=\frac{1}{Pr}(1+\frac{4}{3N})(\frac{\partial^2\theta}{\partial r^2}+\frac{1}{r}\frac{\partial\theta}{\partial z}). \qquad (2.2.3)$$

The boundary conditions (2.1.17) through (2.1.21) become

at $r=r_o(z)$

$$\frac{\partial\Psi}{\partial z}=0 \qquad (2.2.4)$$

$$\frac{\partial\Psi}{\partial r}=0 \qquad (2.2.5)$$

$$\theta = 1 \qquad (2.2.6)$$

for $r \to \infty$

$$\frac{1}{r}\frac{\partial\Psi}{\partial z}\to 0 \qquad (2.2.7)$$

$$\theta \to 0. \qquad (2.2.8)$$

The linear transformation group is defined as

$$z = A^{\alpha 1}z' \qquad (2.2.9)$$

$$r = A^{\alpha 2}r' \qquad (2.2.10)$$

$$\Psi = A^{\alpha 3}\Psi' \qquad (2.2.11)$$

$$\theta = A^{\alpha 4}\theta' \qquad (2.2.12)$$

where

A = parameter of transformation

$\alpha 1, \alpha 2, \alpha 3$, and $\alpha 4$ = constants.

Then momentum equation (2.2.2) is transformed, through the linear group defined in equations (2.2.9) through (2.2.12), as

$$- A^{-\alpha 1+4\alpha 2+2\alpha 3}\frac{1}{r'^2}\frac{\partial\Psi'}{\partial z'}\frac{\partial^2\Psi'}{\partial r'^2} + A^{-\alpha 1+4\alpha 2+2\alpha 3}\frac{1}{r'^3}\frac{\partial^2\Psi'}{\partial r'^2} + A^{-\alpha 1+4\alpha 2+2\alpha 3}\frac{1}{r'^3}\frac{\partial\Psi'}{\partial z'}\frac{\partial\Psi'}{\partial r'}$$

$$+ A^{-\alpha 1+4\alpha 2+2\alpha 3}\frac{1}{r'^2}\frac{\partial\Psi'}{\partial r'}\frac{\partial^2\Psi'}{\partial z'\partial r'}$$

$$= A^{-4\alpha 2+\alpha 3}\frac{1}{r'}\frac{\partial^3\Psi'}{\partial r'^3} - A^{-4\alpha 2+\alpha 3}\frac{1}{r'^2}\frac{\partial^2\Psi'}{\partial r'^2} + A^{-4\alpha 2+\alpha 3}\frac{1}{r'^3}\frac{\partial\Psi'}{\partial r'} - A^{-\alpha 4}\theta'. \quad (2.2.13)$$

Like the momentum equation, the energy equation (2.2.3) is transformed to be

$$- A^{-\alpha 1-2\alpha 2+\alpha 3+\alpha 4}\frac{1}{r'}\frac{\partial\Psi'}{\partial z'}\frac{\partial\theta'}{\partial r'} + A^{-\alpha 1-2\alpha 2+\alpha 3+\alpha 4}\frac{1}{r'}\frac{\partial\Psi'}{\partial r'}\frac{\partial\theta'}{\partial z'} =$$

$$A^{-2\alpha 2+\alpha 4}\frac{1}{Pr}\left(1 + \frac{4}{3N}\right)\left(\frac{\partial^2\theta'}{\partial r'^2} + \frac{1}{r'}\frac{\partial\theta'}{\partial z'}\right). \quad (2.2.14)$$

In order to satisfy the condition of invariancy, the exponent of transformation parameter A must be the same in equations (2.2.13) and (2.2.14), respectively. That condition gives the following relations between the constants:

$$\alpha 3 = \alpha 1, \quad (2.2.15)$$

$$\alpha 1 - 4\alpha 2 = \alpha 4. \quad (2.2.16)$$

The absolute invariants can be obtained by eliminating the parameter A.

$$\eta_1 = rz^t = r'z'^t = A^{-t\alpha 1+\alpha 2}rz^t$$

where

$$t = -\frac{\alpha 2}{\alpha 1}.$$

Hansen [13] showed that any power of an invariant is also an invariant under the same transformation. In this study, we define the new independent variable as a square of η_1.

$$\eta = \left(\frac{r}{z^a}\right)^2 \tag{2.2.17}$$

where

$$a = -\frac{\alpha 2}{\alpha 1}.$$

By the same procedure as η, we obtain similarity stream function f and similarity temperature function g as

$$f(\eta) = \Psi z^s = \Psi' z'^s = A^{-s\alpha 3+\alpha 1}\Psi z^s.$$

By using $\alpha 3 = \alpha 1$ from equation (2.2.15)

$$s = -1$$

$$f(\eta) = \frac{\Psi}{z}, \tag{2.2.18}$$

and

$$g(\eta) = \theta z^m = \theta' z'^m = A^{-m\alpha 3+\alpha 4}\theta z^m.$$

With equation (2.2.16), m can be expressed as

$$m = \frac{\alpha 4}{\alpha 3} = -1 + 4\frac{\alpha 2}{\alpha 1} = -1 + 4a$$

$$g(\eta) = \frac{\theta}{z^{1-4a}}. \tag{2.2.19}$$

Examination of the transformed boundary conditions shows that the boundary conditions can be transformed only if the value of a is specified as $\frac{1}{4}$. This restriction specified the shape of the needle. Define a needle shape parameter η_0 as

$$\frac{r^2}{z^{1/2}} = \eta_0. \tag{2.2.20}$$

The shape of needle is restricted as $r_o(z) = \sqrt{\eta_0 z^{1/2}}$.

Hence, by using the transformation given by equations (2.2.9) through (2.2.12) and by taking $a = \frac{1}{4}$, the momentum equation and energy equation can be transformed into a set of ordinary differential equations. The new independent variable and dependent variables are

$$\eta = \frac{r^2}{z^{1/2}} \tag{2.2.21}$$

$$f(\eta) = \frac{\Psi}{z} \tag{2.2.22}$$

$$g(\eta) = \theta. \tag{2.2.23}$$

The differentiation with respect to r and z can be expressed in terms of η as follows:

$$\frac{\partial}{\partial r} = \frac{2\eta}{r}\frac{\partial}{\partial \eta} \tag{2.2.24}$$

$$\frac{\partial}{\partial z} = -\frac{1}{2}\frac{\eta}{z}\frac{\partial}{\partial \eta}. \tag{2.2.25}$$

Then each of the terms in the momentum and energy equations can be expressed in terms of η as follows:

$$\frac{\partial\Psi}{\partial r} = 2\frac{z}{r}\eta f' \tag{2.2.26}$$

$$\frac{\partial^2\Psi}{\partial r^2} = 2\frac{z}{r^2}\eta f' + 4\frac{z}{r^2}\eta^2 f'' \tag{2.2.27}$$

$$\frac{\partial^3\Psi}{\partial r^3} = 12\frac{z}{r^3}\eta^2 f'' + 8\frac{z}{r^3}\eta^3 f''' \tag{2.2.28}$$

$$\frac{\partial\Psi}{\partial z} = -\frac{1}{2}\eta f' + f \tag{2.2.29}$$

$$\frac{\partial^2\Psi}{\partial z\partial r} = \frac{\eta}{r}f' - \frac{1}{r}\eta^2 f'' \tag{2.2.30}$$

$$\frac{\partial\theta}{\partial r} = \frac{2\eta}{r}g' \tag{2.2.31}$$

$$\frac{\partial^2\theta}{\partial r^2} = 2\frac{\eta}{r^2}g' + \frac{4\eta^2}{r^2}g'' \tag{2.2.32}$$

$$\frac{\partial\theta}{\partial z} = -\frac{1}{2}\frac{\eta}{z}g'. \tag{2.2.33}$$

Then the momentum equation is transformed as follows

$$\text{Left Hand Side} = -\frac{1}{r^2}(-\frac{1}{2}\eta f' + f)(2\frac{z}{r^2}\eta f' + 4\frac{z}{r^2}\eta^2 f'') + \frac{1}{r^3}(-\frac{1}{2}\eta f' + f)(2\frac{z}{r}\eta f')$$
$$+\frac{1}{r^2}(2\frac{z}{r}\eta f')(\frac{\eta}{r}f' - \frac{1}{r}\eta^2 f'') \tag{2.2.34}$$

thus,

$$\text{LHS} = 2\frac{z}{r^4}\eta^2 f^2 - 4\frac{z}{r^4}\eta^2 ff''; \tag{2.2.35}$$

$$\text{Right Hand Side} = 12\frac{z}{r^3}\eta^2 f'' + 8\frac{z}{r^3}\eta^3 f'''$$
$$-\frac{1}{r^2}(2\frac{z}{r^2}\eta f' + 4\frac{z}{r^2}\eta^2 f'') + \frac{1}{r^3}(2\frac{z}{r}\eta f') + \theta \tag{2.2.36}$$

thus,

$$\mathrm{RHS} = 8\frac{z}{r^4}\eta^3 f''' + 8\frac{z}{r^4}\eta^2 f'' + \theta. \tag{2.2.37}$$

Considering equations (2.2.35) and (2.2.37), the following transformed ordinary differential equation for the momentum transport can be obtained as follows:

$$8\eta f''' + 8f'' + 4ff'' - 2f'^2 + g = 0. \tag{2.2.38}$$

The energy equation is transformed as follows:

$$\mathrm{LHS} = \frac{1}{r}\left(-\frac{1}{2}\eta f' + f\right)\left(\frac{2\eta}{r}g'\right) + \frac{1}{r}\left(2\frac{z}{r}\eta f'\right)\left(-\frac{1}{2}\frac{\eta}{z}g'\right) \tag{2.2.39}$$

$$\mathrm{LHS} = \frac{1}{2}\frac{\eta}{r^2}\, fg'; \tag{2.2.40}$$

and

$$\mathrm{RHS} = \frac{1}{\mathrm{Pr}}\left(1 + \frac{4}{3N}\right)\left(4\frac{\eta}{r^2}g' + \frac{4\eta^2}{r^2}g''\right). \tag{2.2.41}$$

Combining equations (2.2.40) and (2.2.41) gives transformed ordinary differential equation for the energy transport

$$\eta g'' + \left[\frac{1}{2}\mathrm{Pr}\frac{1}{1 + \frac{4}{3N}} f + 1\right] g' = 0. \tag{2.2.42}$$

Similarity equations and the boundary conditions are rewritten as

$$8\eta f''' + 8f'' + 4ff'' - 2f'^2 + g = 0 \tag{2.2.38}$$

and

$$\eta g'' + [\frac{1}{2} Pr \frac{1}{1 + \frac{4}{3N}} f + 1]\, g' = 0. \qquad (2.2.42)$$

The boundary conditions (2.2.4) - (2.2.8) become

at $\eta = \eta_0$

$$f(\eta_0) = 0 \qquad (2.2.43)$$

$$f'(\eta_0) = 0 \qquad (2.2.44)$$

$$g(\eta_0) = 1 \qquad (2.2.45)$$

for $\eta \to \infty$

$$f(\eta) \to 0 \qquad (2.2.46)$$

$$g(\eta) \to 0. \qquad (2.2.47)$$

The set of equations (2.2.38) and (2.2.42) with the boundary conditions (2.2.43) - (2.2.47) constitutes similarity equations for natural convection along a needle.

2.3 ANALYSIS OF SIMILARITY EQUATIONS

In this stage, the relation between transformed functions f and g and skin friction factor and heat transfer rate need to be discussed.

Definition of shear stress at the wall is

$$\tau_o = \mu\left(\frac{\partial v_z}{\partial r}\right)_o. \tag{2.3.1}$$

Velocity and length dimension can be transformed into the non-dimensional scaled form by using equations (2.1.11) and (2.1.8) as

$$v_z = v_z\frac{\beta g(T_o - T_\infty)L}{w}$$

$$r = \left(\frac{\nu L}{w}\right)^{1/2} r$$

$$\frac{\partial}{\partial r} = \left(\frac{w}{\nu L}\right)^{1/2}\frac{\partial}{\partial r}. \tag{2.3.2}$$

Shear stress τ_o can be expressed in terms of the non-dimensional scaled variables as

$$\tau_o = \mu\frac{\beta g(T_o - T_\infty)L}{w}\left(\frac{w}{\nu L}\right)^{1/2}\frac{\partial v_z}{\partial r}. \tag{2.3.3}$$

By the equation (2.2.1), $\frac{\partial v_z}{\partial r}$ can be expressed in terms of a stream function

$$\frac{\partial v_z}{\partial r} = -\frac{1}{r^2}\frac{\partial \Psi}{\partial r} + \frac{1}{r}\frac{\partial^2 \Psi}{\partial r^2} \tag{2.3.4}$$

With the equation (2.3.4), shear stress τ_o can be expressed in term of stream function as

$$\tau_o = \mu \frac{\beta g(T_o - T_\infty)L}{w}\left(\frac{w}{\nu L}\right)^{1/2}\left(-\frac{1}{r^2}\frac{\partial \Psi}{\partial r} + \frac{1}{r}\frac{\partial^2 \Psi}{\partial r^2}\right). \tag{2.3.5}$$

With the relation between stream function Ψ and new dependent variable f, which is given in equation (2.2.18), τ_o may be expressed

$$\tau_o = \mu \frac{\beta g(T_o - T_\infty)L}{w}\left(\frac{w}{\nu L}\right)^{1/2}\left[\, 4\frac{z}{r^3}\eta^2 f''\right]_o \tag{2.3.6}$$

$$\tau_o = \mu \frac{\beta g(T_o - T_\infty)L}{w}\left(\frac{w}{\nu L}\right)^{1/2} 4(\eta_o)^{1/2} f''(\eta_o) z^{1/4} \tag{2.3.7}$$

$$\tau_o = \frac{\beta g(T_o - T_\infty)L^3}{\nu^2}\frac{1}{(Re)^{5/2}}\rho w^2\, 4(\eta_o)^{1/2} f''(\eta_o) z^{1/4} \tag{2.3.8}$$

$$\tau_o = Gr\frac{1}{(Re)^{5/2}}\frac{1}{2}\rho w^2\, 8(\eta_o)^{1/2} f''(\eta_o) z^{1/4} \tag{2.3.9}$$

$$\frac{\tau_o}{\frac{1}{2}\rho w^2}\frac{(Re)^{5/2}}{Gr} = 8(\eta_o)^{1/2} f''(\eta_o) z^{1/4}. \tag{2.3.10}$$

Average shear stress can be expressed as

$$\overline{\tau_o} = \frac{1}{z_L}\int_o^{z_L} \tau_o(z)\, dz. \tag{2.3.11}$$

Substituting $\tau_o(z)$ in equation (2.3.10) into equation (2.3.11) gives

$$\overline{\tau}_o = \frac{1}{z_L}\int_o^{z_L} Gr \frac{1}{(Re)^{5/2}} \frac{1}{2}\rho w^2 \, 8(\eta_o)^{1/2} f''(\eta_o) z^{1/4} dz \qquad (2.3.12)$$

where z_L represents characteristic length in **z** dimension and z_L can be expressed as

$$z_L = \left[\frac{w^2}{\beta g(T_o - T_\infty)L}\frac{z}{L}\right]_{(at\ z\ =\ L)} = \frac{v^2}{\beta g(T_o - T_\infty)L^3}\frac{L^2}{v^2} w^2 \qquad (2.3.13)$$

$$z_L = \frac{1}{Gr}(Re)^2. \qquad (2.3.14)$$

After performing integration in equation (2.3.12), the average shear stress $\overline{\tau}_o$ is shown as

$$\overline{\tau}_o = Gr \frac{1}{(Re)^{5/2}} \frac{1}{2}\rho w^2 \frac{32}{5}(\eta_o)^{1/2} f''(\eta_o)(z_L)^{1/4}. \qquad (2.3.15)$$

Simplifying equation (2.3.15) shows that the average shear stress may be expressed as

$$\overline{\tau}_o = (Gr)^{3/4} \frac{1}{(Re)^2} \frac{1}{2}\rho w^2 \frac{32}{5}(\eta_o)^{1/2} f''(\eta_o) \qquad (2.3.16)$$

$$\frac{\overline{\tau}_o}{\frac{1}{2}\rho w^2}\frac{(Re)^2}{(Gr)^{3/4}} = \frac{32}{5}(\eta_o)^{1/2} f''(\eta_o). \qquad (2.3.17)$$

Equation (2.3.17) shows that $f''(\eta_o)$ is related to the skin friction factor.

The heat flux at the wall is defined by

$$q_o = -k\,\left(\frac{\partial T}{\partial \mathbf{r}}\right)_o. \tag{2.3.18}$$

By using the relationship between $\mathbf{r}$ and r, $r = (Re)^{1/2}\frac{\mathbf{r}}{L}$, equation (2.3.18) is transformed as

$$q_o = -k\,\left(\frac{\partial T}{\partial r}\right)_o\left(\frac{w}{\nu L}\right)^{1/2}. \tag{2.3.19}$$

Non-dimensional temperature is defined as

$$\theta = \frac{T - T_\infty}{T_o - T_\infty} \tag{2.1.15}$$

$$\text{So, } \frac{\partial T}{\partial r} = \frac{\partial \theta}{\partial r}(T_o - T_\infty)$$

$$\frac{\partial \theta}{\partial r} = \frac{2\eta}{r}\, g'. \tag{2.3.20}$$

With equation (2.1.15) and (2.3.20), equation (2.3.19) may be rewritten as

$$q_o = -2k\frac{T_o - T_\infty}{L}\,(Re\eta_o)^{1/2}\frac{g'(\eta_o)}{z^{1/4}}. \tag{2.3.21}$$

The average heat flux at the wall is defined as

$$\overline{q_o} = \frac{1}{z_L}\int_o^{z_L} q_o(z)\,dz \qquad (2.3.22)$$

$$\overline{q_o} = \frac{1}{z_L}\int_o^{z_L} -2k\frac{T_o - T_\infty}{L}(Re\eta_o)^{1/2}\frac{g'(\eta_o)}{z^{1/4}}dz \qquad (2.3.23)$$

$$\overline{q_o} = -\frac{8}{3}k\frac{T_o - T_\infty}{L}(Re\eta_o)^{1/2}g'(\eta_o)\frac{1}{z^{1/4}_L}. \qquad (2.3.24)$$

Substituting z_L into equation (2.3.24) gives

$$\overline{q_o} = -\frac{8}{3}k\frac{T_o - T_\infty}{L}(\eta_o)^{1/2}g'(\eta_o)(Gr)^{1/4}. \qquad (2.3.25)$$

This average heat transfer rate can be expressed in terms of an average Nusselt number.

Average Nusselt number is defined as

$$\overline{Nu} = \frac{\overline{h}L}{k}$$

where

$\overline{h}$ = average heat transfer coefficient ($= \frac{\overline{q_o}}{\Delta T}$)

$$\overline{Nu} = -\frac{8}{3}(\eta_o)^{1/2}g'(\eta_o)(Gr)^{1/4} \qquad (2.3.26)$$

$$\frac{\overline{Nu}}{(Gr)^{1/4}} = -\frac{8}{3}(\eta_o)^{1/2}g'(\eta_o). \qquad (2.3.27)$$

Equation (2.3.27) shows the relationship between $g'(r_o)$ and the heat transfer rate at the wall.

CHAPTER III

ANALYSIS OF THE SIMILARITY SOLUTION

3.1 GENERAL FEATURE OF THE SHOOTING METHOD

From the previous chapter, the similarity equations for boundary layer equations in natural free convection with radiation effect were obtained as

$$8\eta f''' + 8f'' + 4ff'' - 2f'^2 + g = 0 \qquad (2.2.38)$$

$$\eta g'' + [\frac{1}{2}\Pr\frac{1}{1+\frac{4}{3N}}f + 1]\, g' = 0 \qquad (2.2.42)$$

at $\eta = \eta_0$

$$f(\eta_0) = 0 \qquad (2.2.43)$$

$$f'(\eta_0) = 0 \qquad (2.2.44)$$

$$g(\eta_0) = 1 \qquad (2.2.45)$$

for $\eta \rightarrow \infty$

$$f(\eta) \rightarrow 0 \qquad (2.2.46)$$

$$g(\eta) \rightarrow 0. \qquad (2.2.47)$$

Whole structure of the above equations reveals they are a highly non-linear and coupled equations which make it almost impossible to obtain analytical solutions. Also examination of the above equations shows that the boundary conditions are described at infinity.

In spite of the difficulties involved in the solution of this type of equation, an excellent result can be obtained through the use of numerical techniques. The technique employed in this study was the shooting method. This method uses an initial guess for unspecified initial conditions.

Proceeding with those initial guesses, it integrates values of each functions and examines whether it satisfies prescribed boundary conditions at infinity. If the calculated values diverge, it automatically adjusts its initial guess until it satisfies the boundary conditions at infinity.

3.2 SATISFACTION OF ASYMPTOTIC BOUNDARY CONDITIONS

The nature of the restriction imposed on both the momentum and energy equations by the boundary conditions involved ($\eta \to \infty$, $f(\eta) \to 0$, $g(\eta) \to 0$) indicates an asymptotic approach to a limiting value of zero for these functions. The method of Nachtsheim and Swigert [6] provides a means for predicting the amount of error in initial guesses for the starting values used in the numerical solution of differential equations which include asymptotic boundary conditions. Knowledge of the magnitude of this error then allows adjustment or correction of the initial guesses to a degree commensurate with the limits of accuracy desired for the problem.

The asymptotic boundary conditions are replaced by the conditions that $f'(\eta) = 0$ and $g(\eta) = 0$ to a sufficient degree of accuracy at $\eta = \eta_{edge}$, where η_{edge} is the value of the independent variable at the edge of the boundary layer. The above boundary value problem is equivalent to the problem to find values of $f''(\eta_0)$ and $g'(\eta_0)$ for which the boundary conditions at the edge of the boundary layer are satisfied.

$$f'_{edge}[\, f''(\eta_0)] = 0. \tag{3.2.1}$$

$$g_{edge}[\, g'(\eta_0)] = 0. \tag{3.2.2}$$

Let the initial guesses

$$f''(\eta_0) = x \tag{3.2.3}$$

$$g'(\eta_0) = z. \tag{3.2.4}$$

Changing x and z changes f' and g by the amount of

$$\frac{\partial f'}{\partial x}\Delta x \text{ and } \frac{\partial g}{\partial z}\Delta z,$$

so that the necessary correction to a first approximation comes from the solution of the linear equations

$$0 = f' + \frac{\partial f'}{\partial x}\Delta x + \frac{\partial f'}{\partial z}\Delta z \text{ and} \tag{3.2.5}$$

$$0 = g + \frac{\partial g}{\partial x}\Delta x + \frac{\partial g}{\partial z}\Delta z \text{ at } \eta_{edge}. \tag{3.2.6}$$

In order to satisfy the asymptotic boundary conditions, the above equation must be supplemented by

$$0 = f'' + f''_x\Delta x + f''_z\Delta z \tag{3.2.7}$$

$$0 = g' + g'_x\Delta x + g'_z\Delta z \tag{3.2.8}$$

where $f'_x = \frac{\partial f'}{\partial x}$, $f''_x = \frac{\partial f''}{\partial x}$, etc

The solution of the equation for Δx and Δz can be performed provided that the partial derivative of f' with respect to x and the partial derivative of g with respect to z can be evaluated at η_{edge}. Using the concept of least square, Δx and Δz must be found such that the sum of squares of the preceding four equations is minimum value. Let be

$$\delta_1 = f' + \frac{\partial f'}{\partial x}\Delta x + \frac{\partial f'}{\partial z}\Delta z, \tag{3.2.9}$$

$$\delta_2 = g + \frac{\partial g}{\partial x}\Delta x + \frac{\partial g}{\partial z}\Delta z, \tag{3.2.10}$$

$$\delta_3 = f'' + f''_x\Delta x + f''_z\Delta z, \tag{3.2.11}$$

$$\delta_4 = g' + g'_x\Delta x + g'_z\Delta z. \tag{3.2.12}$$

Let $S = \delta_1{}^2 + \delta_2{}^2 + \delta_3{}^2 + \delta_4{}^2$ be minimum by taking partial derivatives of S with respect to x and z and equating each partial derivative to zero. That gives the following matrix equation.

$$\begin{bmatrix} f'^2_x + g^2_x + f''^2_x + g'^2_x, & f'_x f'_z + g_x g_z + f''_x f''_z + g'_x g'_z \\ f'_x f'_z + g_x g_z + f''_x f''_z + g'_x g'_z, & f'^2_z + g^2_z + f''^2_z + g'^2_z \end{bmatrix} \begin{bmatrix} \Delta x \\ \Delta z \end{bmatrix}$$
$$= -\begin{bmatrix} f'f'_x + gg_x + f''f''_x + g'g'_x \\ f'f'_z + gg_z + f''f''_z + g'g'_z \end{bmatrix}. \tag{3.2.13}$$

The values of x and z that give $\Delta x = \Delta z = 0$ correspond to the minimum with respect to x and z of the quantity

$$E = f'^2 + g^2 + f''^2 + g'^2 . \tag{3.2.15}$$

The partial derivative can be evaluated by forming the set of perturbation equations for the function f' and g for the x derivatives. With the notation

$$f_x = \frac{\partial f}{\partial x}, \quad f'_x = \frac{\partial f'}{\partial x}, \ldots$$
$$g_x = \frac{\partial g}{\partial x}, \quad g'_x = \frac{\partial g'}{\partial x}, \ldots$$

the following set of perturbation equations are obtained:

$$8\eta f'''_x + 8f''_x + 4f_x f'' + 4ff''_x - 4f'f'_x + g_x = 0 \qquad (3.2.16)$$

and

$$\eta g''_x + \left[\frac{1}{2}\mathrm{Pr}\frac{1}{1+\frac{4}{3N}} f + 1\right] g'_x + \frac{1}{2}\mathrm{Pr}\frac{1}{1+\frac{4}{3N}} f_x g' = 0 \qquad (3.2.17)$$

with the initial conditions

at $\eta = \eta_o$

$$f_x = 0 \qquad (3.2.18)$$

$$f'_x = 0 \qquad (3.2.19)$$

$$g_x = 0 \qquad (3.2.20)$$

$$g'_x = 0 \qquad (3.2.21)$$

$$f''_x = 1. \qquad (3.2.22)$$

The perturbation equations for z derivatives are

$$8\eta f'''_z + 8f''_z + 4f_z f'' + 4ff''_z - 4f'f'_z + g_z = 0 \qquad (3.2.23)$$

and

$$\eta g''_z + \left[\frac{1}{2}\mathrm{Pr}\frac{1}{1+\frac{4}{3N}} f + 1\right] g'_z + \frac{1}{2}\mathrm{Pr}\frac{1}{1+\frac{4}{3N}} f_z g' = 0 \qquad (3.2.24)$$

With the initial conditions

at $\eta = \eta_o$

$$f_z = 0 \qquad (3.2.25)$$

$$f'_z = 0 \qquad (3.2.26)$$

$$f''_z = 0 \qquad (3.2.27)$$

$$g_z = 0 \qquad (3.2.28)$$

$$g'_z = 1. \qquad (3.2.29)$$

By changing problems from the boundary values problem to the initial value problem, it is possible to solve the whole set of equations by using many available subroutines. In this study, the method used by Nachtsheim and Swigert was employed to solve a set of equations.

The general feature of that algorithm may be summarized as follows: Given initial estimate of $x = f''(\eta_o)$ and $z = g'(\eta_o)$, subsequent values of x and z can be computed by integrating equations (2.2.38), (2.2.42) through (2.2.47) , (3.2.16) through (3.2.22) , (3.2.23) through (3.2.29) and applying the Newton-Raphson method to obtain corrections.

The problem of where to stop the integration was determined by calculating the error E at each step . If E is smaller than the prescribed allowance, it stops and takes the value of η as η_{edge}

3.3 RESULT OF THE SOLUTION ALGORITHM

The method used by Nachtsheim and Swigert was employed because it is stable in a sense that it is insensitive to initial guesses, and the error term is well controlled. The computer program obtains values from a starting point, where the corrections to the initial guesses for $f''(\eta_o)$ and $g'(\eta_o)$ apply. The error derived in section 3.2 is calculated at η_{edge} and the solution convergence is checked. If the calculated error is larger than the desired error, the magnitude of η_{edge} is increased and the initial guesses are corrected. The new value for η_{edge} and corrected initial guesses for $f''(\eta_o)$ and $g'(\eta_o)$ are then used to solve the equations until the boundary conditions, error limits, and solution convergence requirements are met.

The integration was carried out to an assumed end of the boundary layer, η_{edge}. The initial guess for η_{edge} was 4.0 which was increased by 2.0 until the convergence was achieved and the error requirement was met. The maximum error used in the analysis is 10^{-5}. The initial guesses for $f''(\eta_o)$ and $g'(\eta_o)$ were 1.0 and -5.0, respectively.

Fig. 2 through Fig. 13 show the results of the solution algorithm. Fig. 2 through Fig. 7 show the relationship between needle shape factor and the transformed skin friction factor as well as the transformed heat transfer rate for Prandtl numbers = 1, 10, 100. Fig. 8 through Fig. 13 show transformed velocity and temperature profiles. Specifically, Fig. 8 through Fig. 11 show both velocity and temperature profiles for $\eta_o = 0.001$ and 0.1 as Pr = 1, 10, 100 with no radiation case, while Fig. 12 through Fig. 13 show both the profile for $\eta_o = 0.1$ and $N = \infty$, 1.0, 0.1 with Pr = 10.0.

Examinations of Fig. 2 through Fig. 4 give several trends in behavior of skin friction factor as to changing values of Prandtl numbers, the degree of radiation and needle shape which was magnified by η_o. First, the more slender needle increases the skin friction factor. Secondly, higher Prandtl numbers indicates larger thermal boundary layer than the momentum boundary layer and a decreased skin friction factor. Finally, an increased degree of radiation increases the skin friction factor especially with a high Prandtl number.

Some observations of Fig. 4 through Fig. 7 readily show several trends in heat transfer rate according to changing values of needle shape parameters, Prandtl number, and degree of radiation. First, the more slender needle shows the higher heat transfer rate. Secondly, with higher Prandtl numbers, which mean higher thickness of thermal boundary layer than that of momentum boundary layer, the rate of heat transfer increases. Finally, an increased degree of radiation decreases heat transfer rate.

Several observations can be made from Fig. 8 through Fig. 11. For velocity profile, the higher Prandtl number increases the value of maximum velocity and momentum boundary layer. For temperature profile, the higher Prandtl number increases the thermal boundary layer.

From examining Fig. 12 through Fig. 13, with more radiation, both the value of maximum velocity and thickness of momentum boundary layer are increased, and the thickness of thermal boundary layer is also increased.

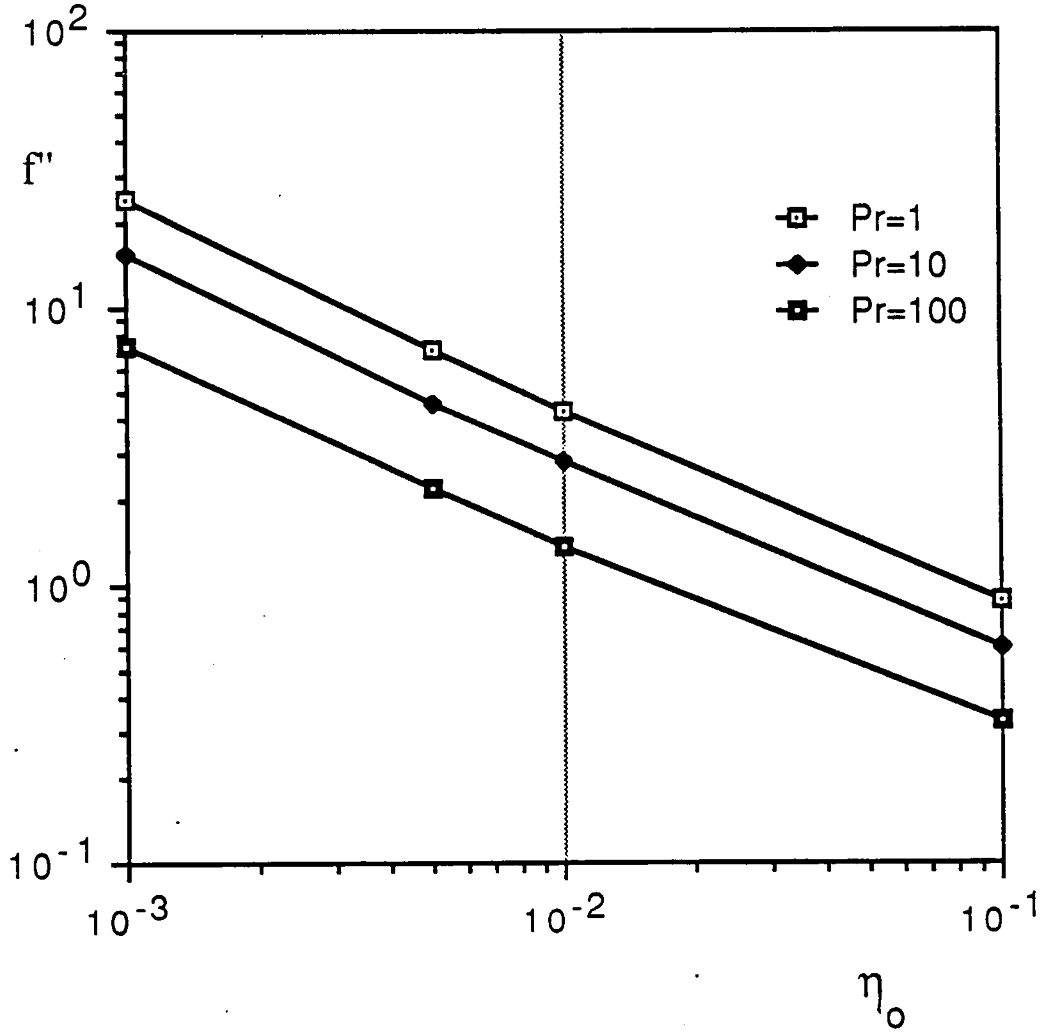

Fig. 2. Transformed skin friction $f''(\eta_o)$ vs. needle shape parameter η_o

with no-radiation

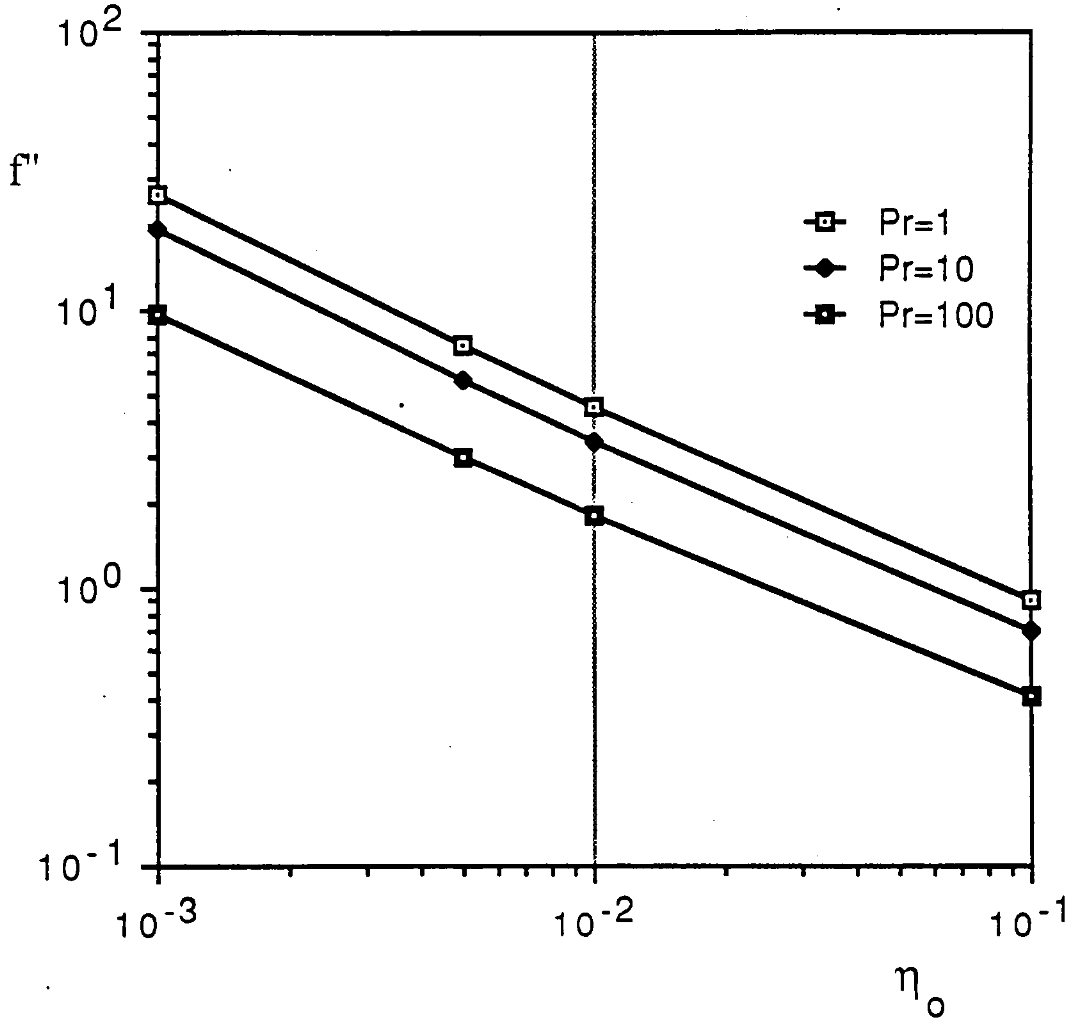

Fig. 3. Transformed skin friction $f''(\eta_o)$ vs. needle shape parameter η_o

N (conduction to radiation ratio) = 1.0

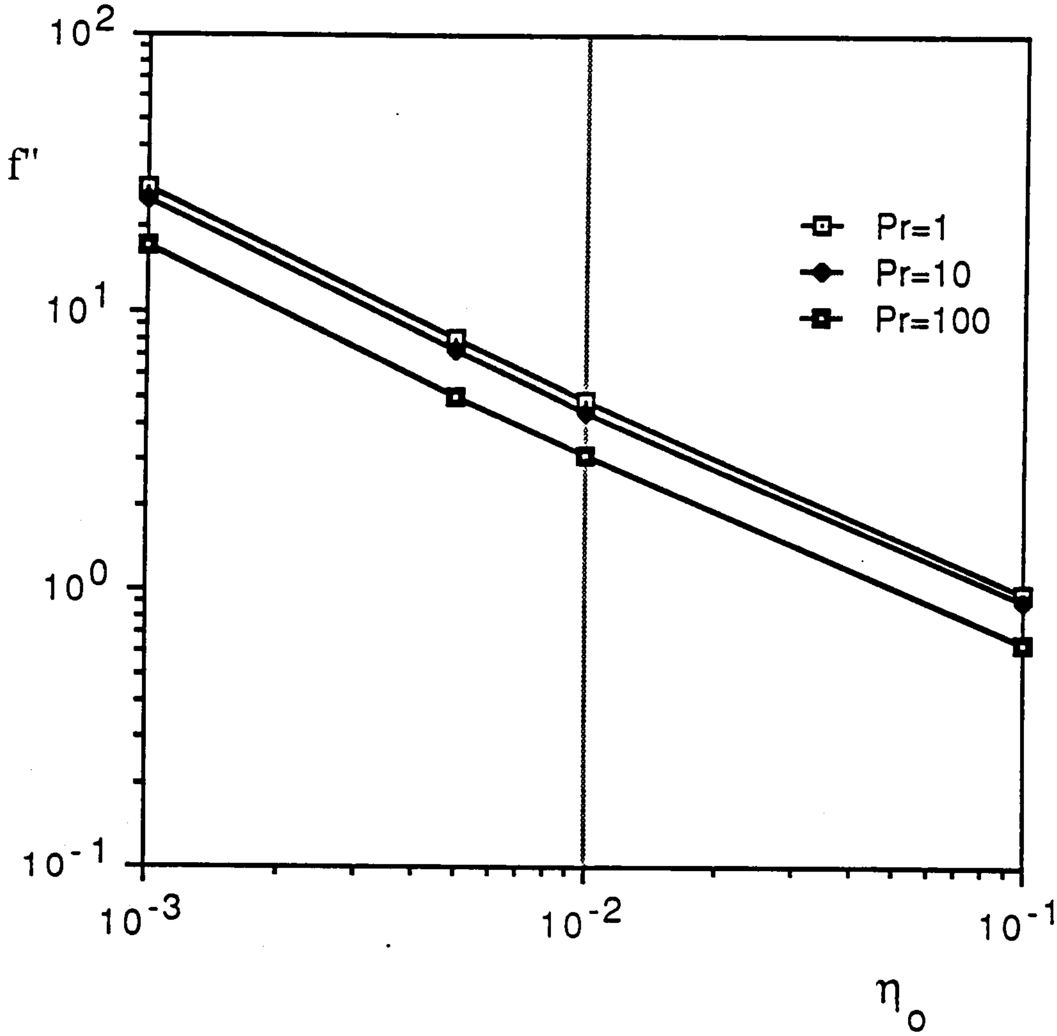

Fig. 4. Transformed skin friction $f''(\eta_o)$ vs. needle shape parameter η_o

N (conduction to radiation ratio) = 0.1

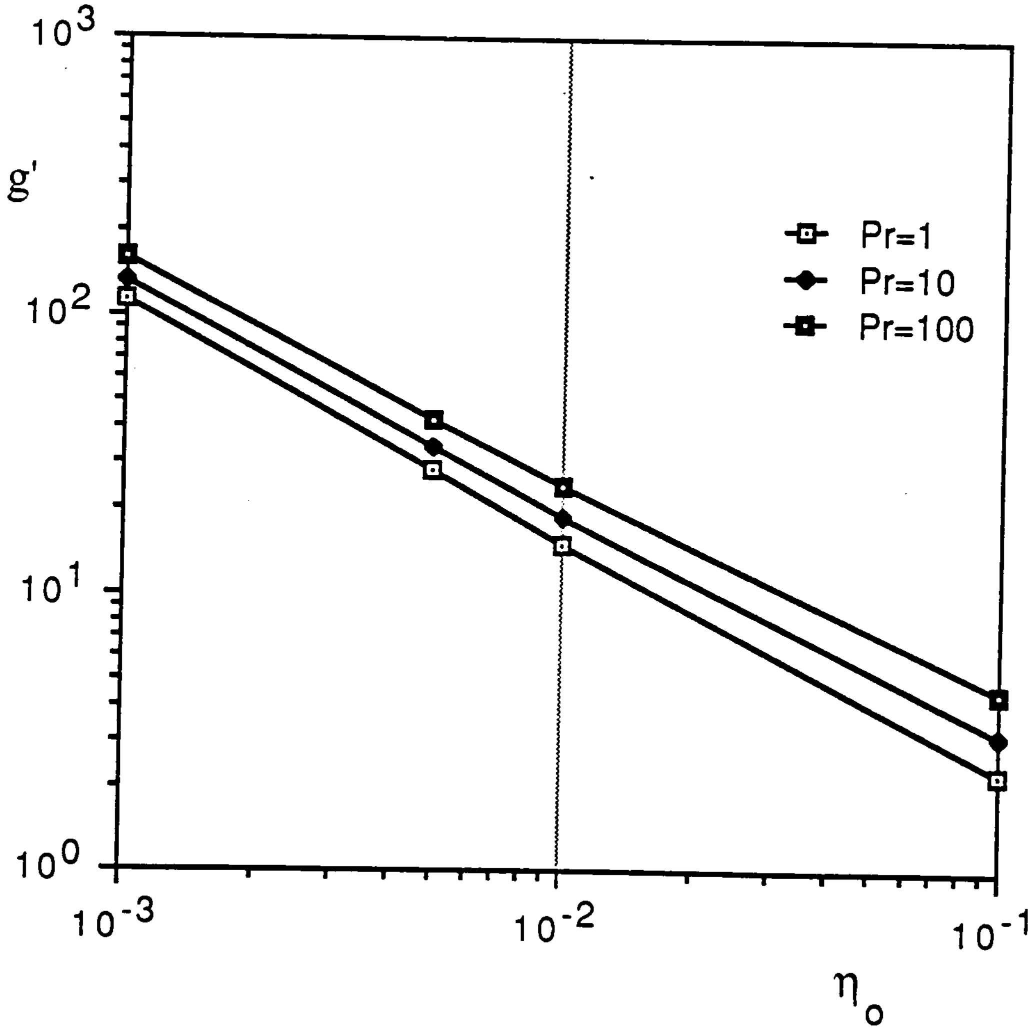

Fig. 5. Transformed heat transfer rate $g'(\eta_o)$ vs. needle shape parameter η_o with no-radiation

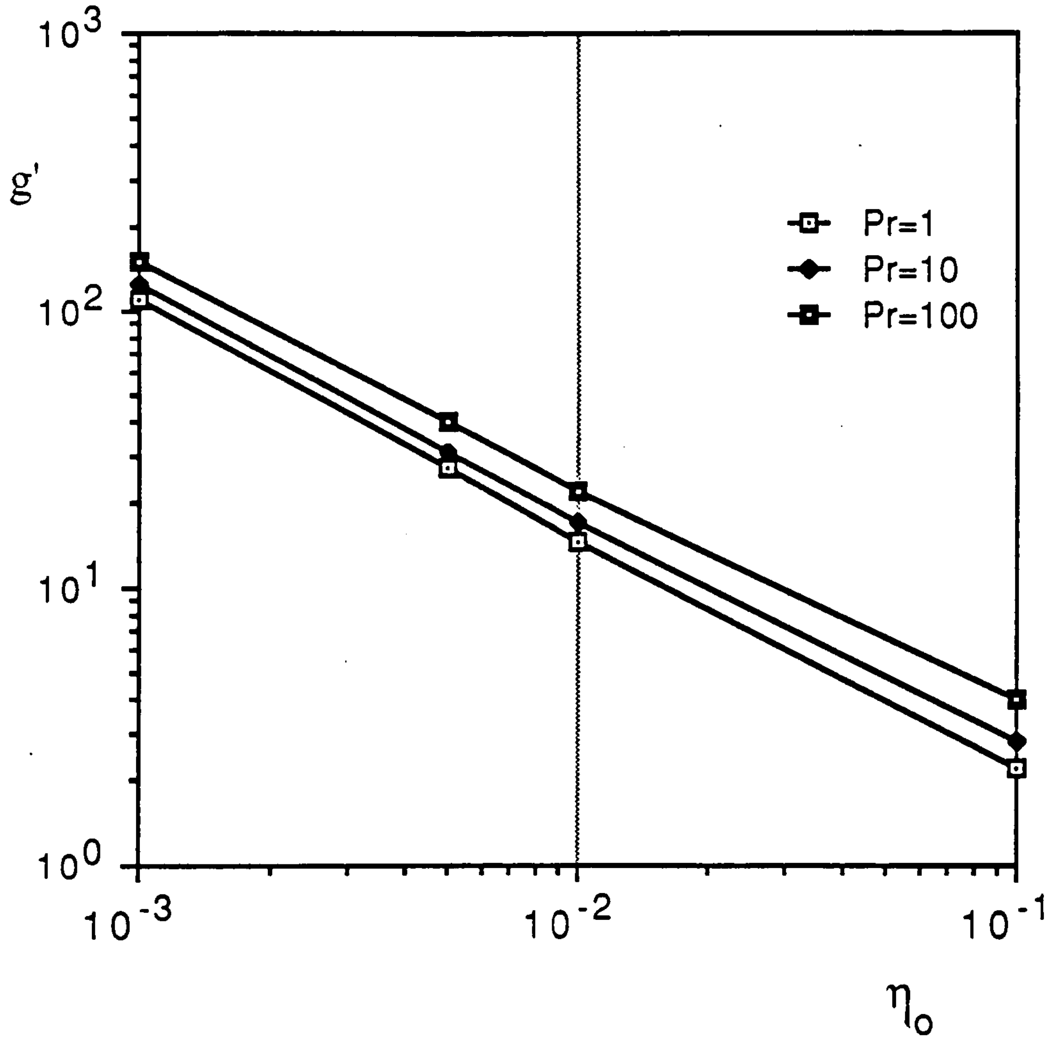

Fig. 6. Transformed heat transfer rate $g'(\eta_o)$ vs. needle shape parameter η_o

with N (conduction to radiation ratio) = 1.0

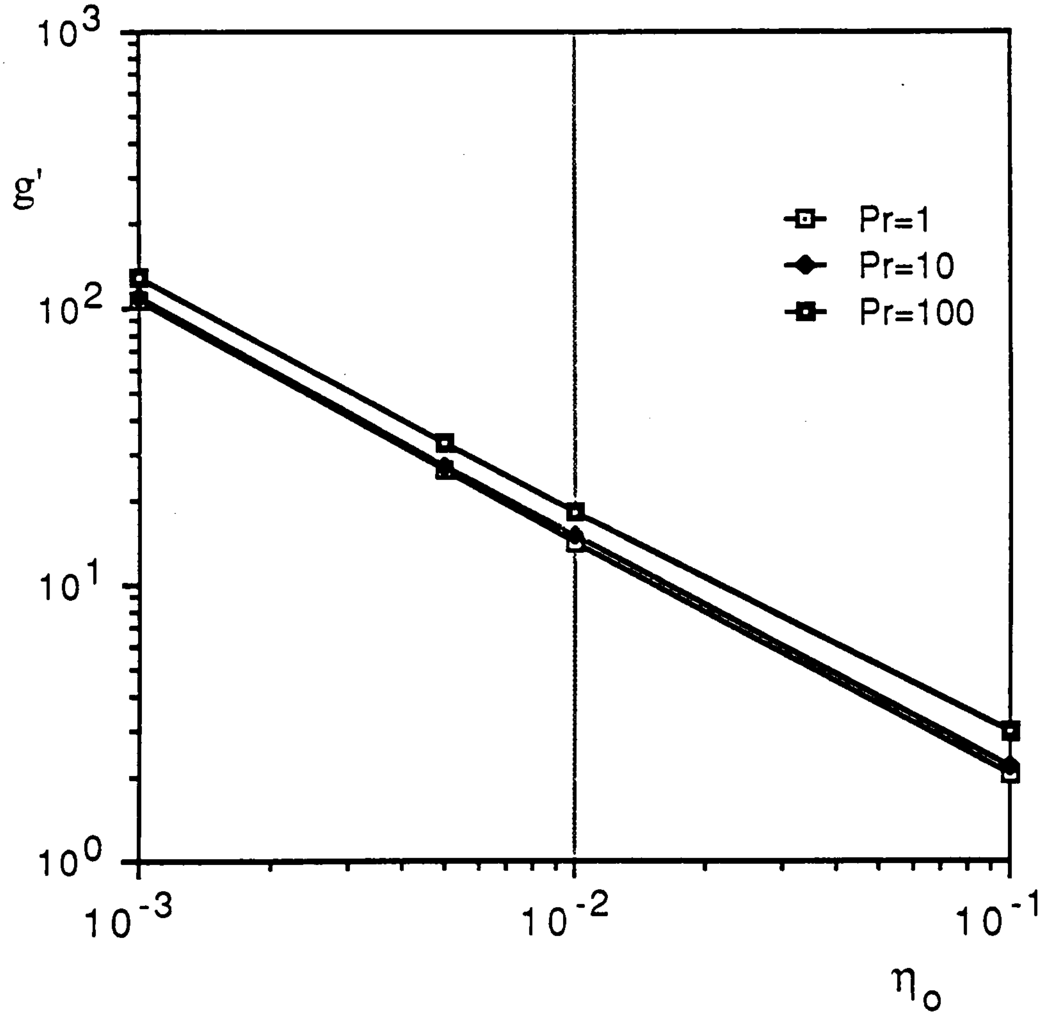

Fig. 7. Transformed heat transfer rate $g'(\eta_o)$ vs. needle shape parameter η_o

with N (conduction to radiation ratio) = 0.1

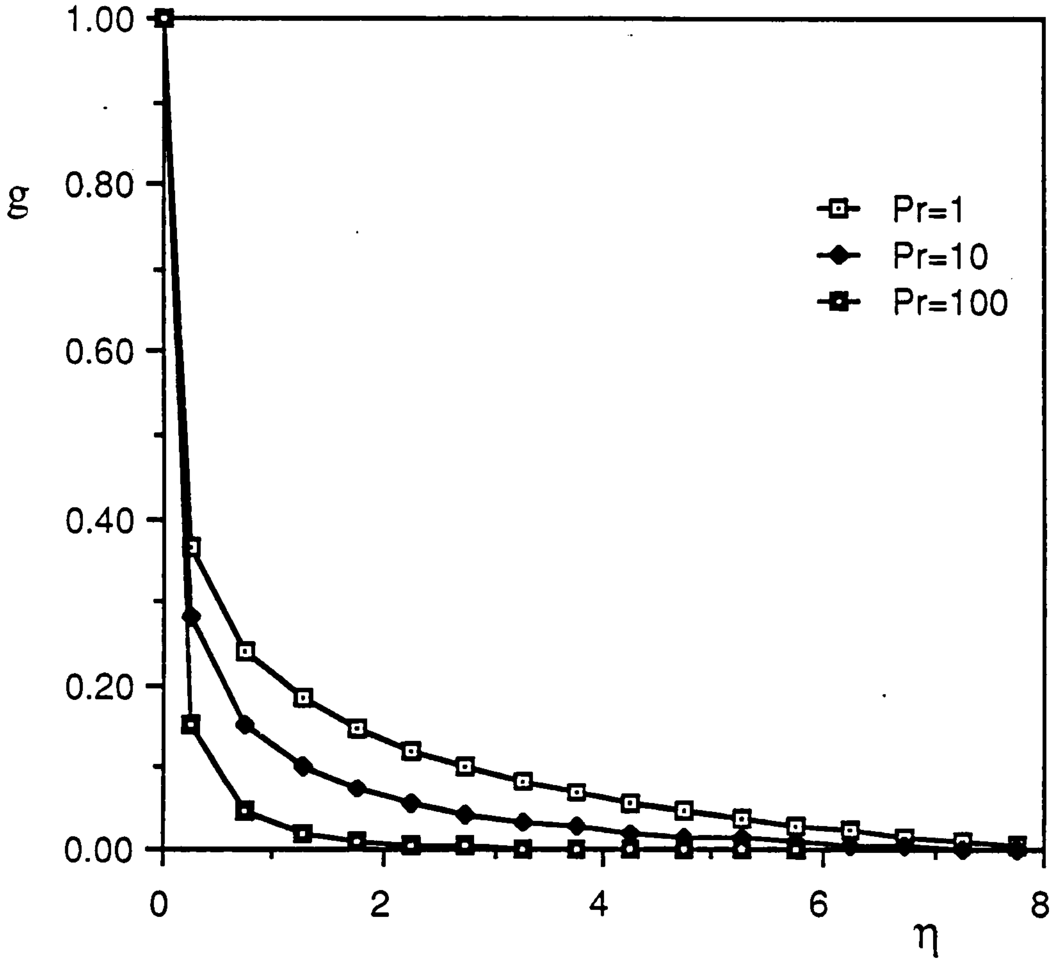

Fig. 8. Similarity temperature profile

with $\eta_o = 0.001$ and no-radiation

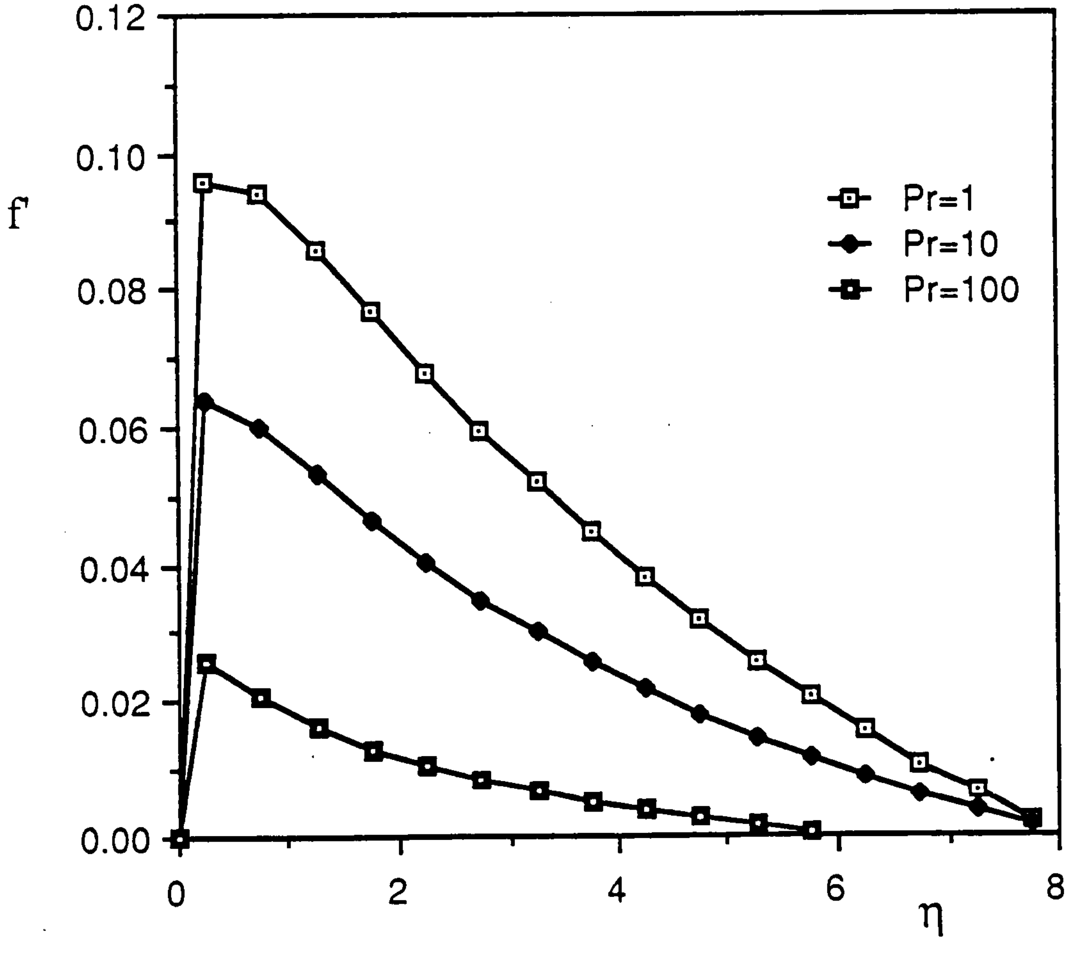

Fig. 9. Similarity velocity profile

with $\eta_o = 0.001$ and no-radiation

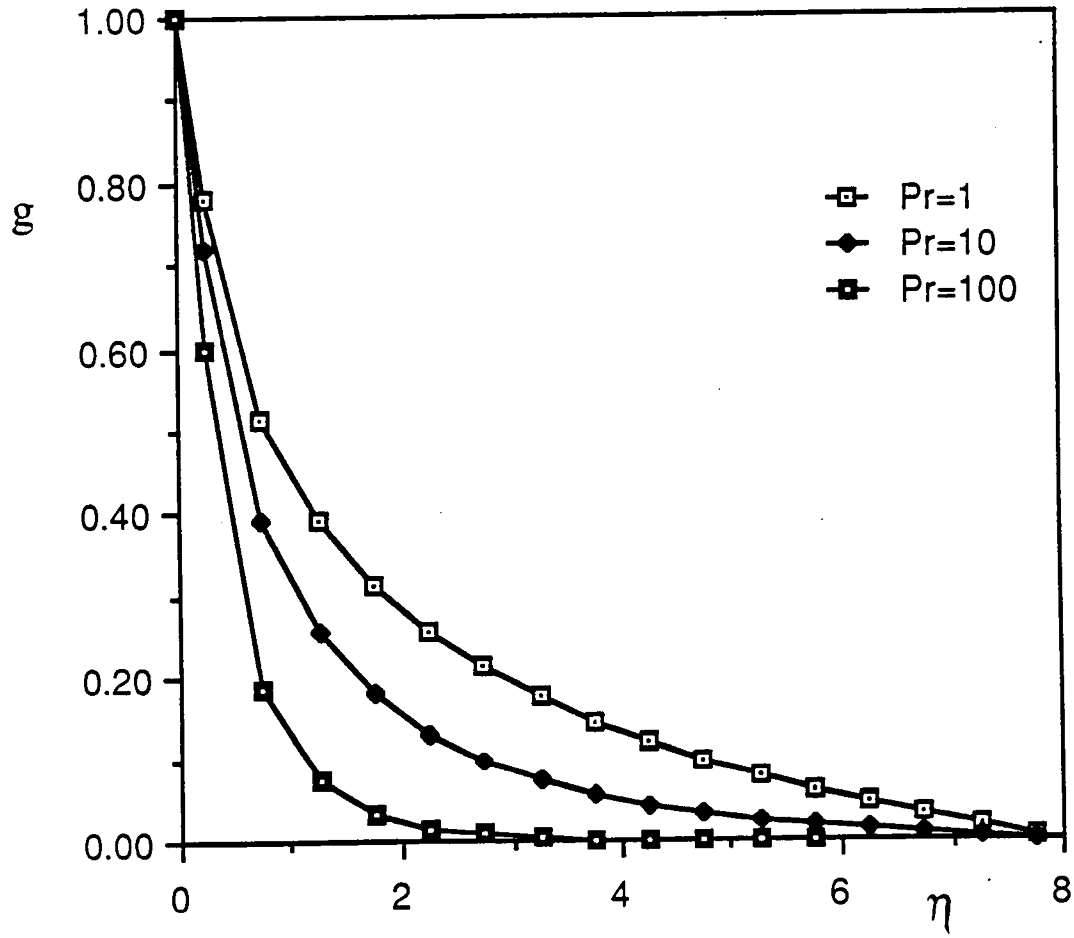

Fig. 10. Similarity temperature profile

with $\eta_o = 0.1$ and no-radiation

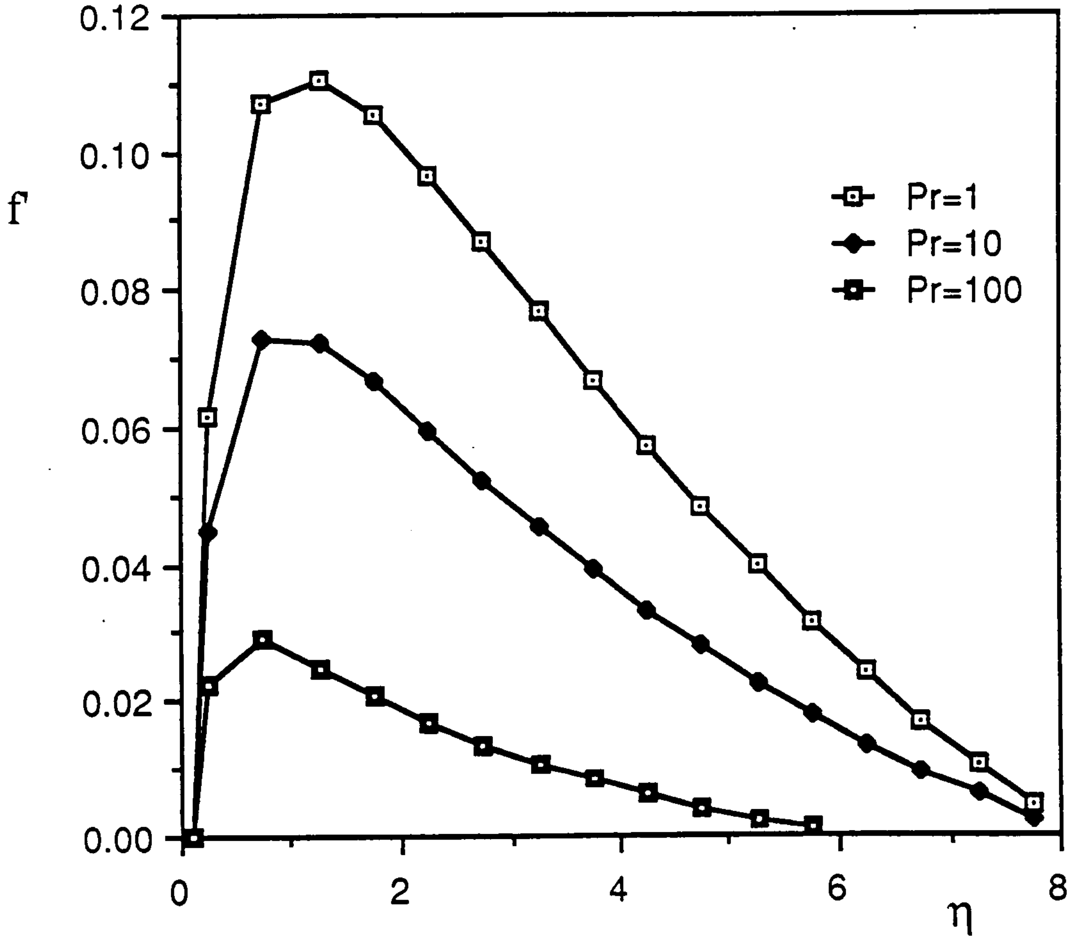

Fig. 11. Similarity velocity profile

with η_o =0.1 and no-radiation

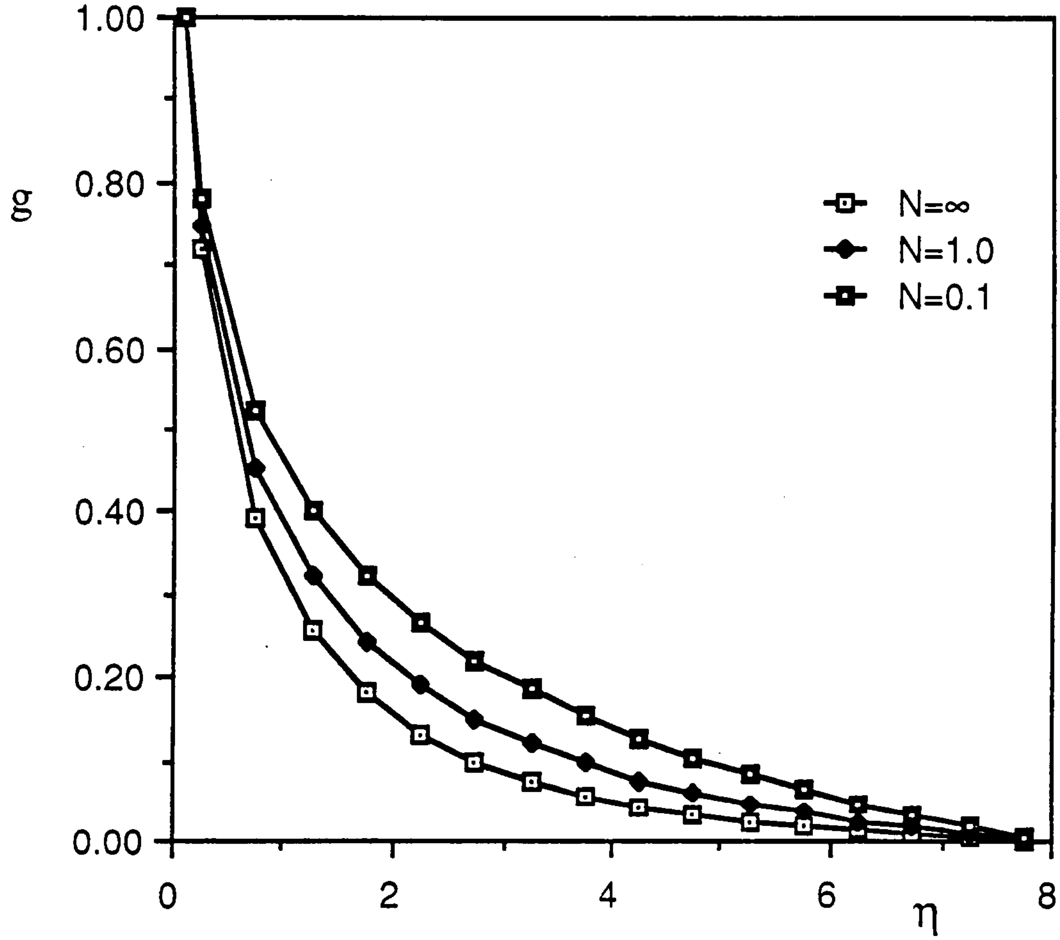

Fig. 12. Similarity temperature profile

with $\eta_o = 0.1$ and Prandtl number = 10.0

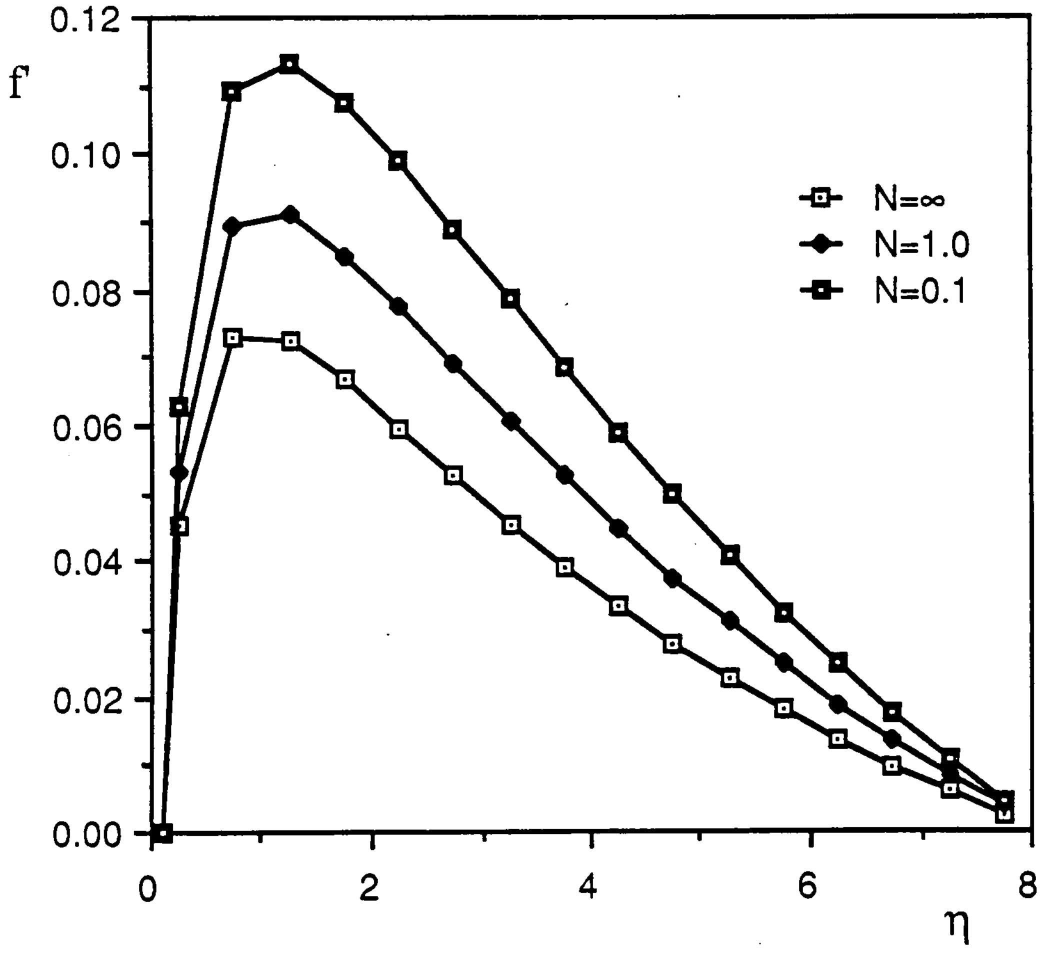

Fig. 13. Similarity velocity profile

with $\eta_o = 0.1$ and Prandtl number = 10.0

CHAPTER IV

CONCLUSION AND RECOMMENDATIONS

The finding of this study provides information which can be used to examine a laminar boundary layer under the influence of natural convection with radiation heat transfer.

The effects of the needle shape and thermal radiation upon a laminar free convection along an isothermal slender needle were studied. The set of boundary layer equations were transformed through the linear transformation group which produced ordinary differential forms of the momentum and energy equations. For the radiative heat flux term, the simplification was made through the Rosseland approximation by assuming an optically thick medium. Then the temperature term was linearized through the Taylor expansion method. The momentum and energy equations were numerically solved by predicting the missing initial conditions and examining the satisfaction of boundary conditions at the edge. The numerical results were calculated for three values of Prandtl numbers for 1, 10, 100 and three values of N, the conduction to radiation ratio, for ∞, 1.0, 0.1.

This result was compared to that of Cebeci [2] who calculated the effect of the needle shape upon the skin friction and the heat transfer rate without considering the radiation effect. This study agrees with Cebeci by setting $N = \infty$. The results of this study show the effect of the needle shape parameter upon the transformed skin friction and the transformed heat transfer rate as well as the transformed velocity and temperature profile in the boundary layer. Those results can be reduced to the following conclusions:

1. The needle shape affects both the skin friction and the heat transfer rate, which were increased as the needle became more slender.

2. The Prandtl number affects both the skin friction and the heat transfer rate. As the Prandtl number was increased, the skin friction factor was decreased while the heat transfer rate was increased. This is physically plausible because the Prandtl number is a representation of the ratio of the thermal boundary layer thickness to the momentum boundary layer thickness, therefore the higher Prandtl number indicates that the thickness of the thermal boundary layer is greater than the momentum boundary layer.

3. The radiation affects the thickness of the momentum and thermal boundary layers. As the radiation heat transfer became dominant, the heat distribution became more evenly spread out in the fluid boundary layer, and the maximum velocity of the fluid was increased. This can be explained in two ways. First, through an optically thick assumption the radiative heat flux term can be considered as a diffusion process, therefore the higher radiation means more diffusive energy and momentum transport among the medium. Second, the conduction process occurs by temperature differences while the radiation takes place at relatively high temperatures. Since N, the conduction to radiation ratio, is expressed by the ratio of conduction to radiation terms, the higher N means that high temperatures condition is dominant over temperature differences condition.

Further research is required to extend this study. For example, the study of a pair of needles could give valuable information for a bundle of hot wires. Additional refinement will be needed to increase the accuracy of a radiative heat flux term without losing the requirement for similarity transformations.

LIST OF REFERENCES

LIST OF REFERENCES

1. Narain, J. P., and Uberoi, M. S. , " Laminar Free Convection from Vertical Thin Needles," The Physics of Fluids, Vol. 15, No. 5, pp. 928 - 929, 1972.

2. Cebeci, T., and Na, T. S., " Laminar Free-Convection Heat Transfer from a Needle," The Physics of Fluids, Vol. 12, No. 3, pp. 463 - 467, 1969.

3. Narain, J. P., " Free and Forced Convective Heat Transformation Slender Cylinders", Letters in Heat and Mass Transfer, Vol. 3, 1976, pp. 21 - 30

4. Raithby, G. D., et al., " Free Convection Heat Transfer from Spheroids," Journal of Heat Transfer, pp. 452 - 458, August 1976.

5. Sparrow, E. M., and Cess, R. D., Radiation Heat Transfer, 1st ed., Brooks/Cole Publishing: Belmont, California, 1966.

6. Nachtsheum, P. R., and Swigert, P., "Satisfaction of Asymptotic Boundary Conditions in Numerical Solution of Systems of Non-linear Equations of Boundary Layer Type," NASA Technical Note D3004, National Aeronautics and Space Administration, 1965.

7. Viskanta, R., and Grosh, R. J., " Boundary Layer in Thermal Radiation Absorbing and Emitting Media," International Journal of Heat and mass Transfer, Vol. 5, pp. 795 - 806, 1962.

8. Kim, K. H., Ozisik, M. N., and Mulligan, J. C., " A Non-Similar Solution of Heat Transfer in External Non-Newtonian Flow with Thermal Radiation," AIAA Paper No. 73-116, 1973.

9. Novotny, J. L., and Yang, K. T. " The Interaction of Thermal Radiation in Optically Thick Boundary Layers," ASME Paper No. 67 HT-9, 1967.

10. Goulard, R., " The Transition from Blackbody to Rosseland Formulations in Optically Thick Flows," International Journal of Heat and Mass Transfer, Vol. 7, pp. 1145 - 1146, 1964.

11. Kim, K. H., and Ozisik, M. N., " Application of Normal-Mode-Expansion Technique to Absorbing, Emitting, and Scattering Stagnation Point Boundary Layer Flow," Development in Theoretical and Applied Mechanics, Proceeding of the Tenth Southeastern Conference on Theoretical and Applied Mechanics, Vol. 10, pp. 681, 1980.

12. Raithby, G. D. and Hollands, K. G. T. " Free Convection Heat Transfer from Vertical Needles," Journal of Heat Transfer, pp. 522 - 523, August 1976.

13. Hansen, A. G., Similarity Analyses of Boundary Value Problems in Engineering, Prentice Hall: Englewood Cliffs, NJ, 1964.

VITA

Guy H. Lee was born in Seoul, Korea on September 3, 1960. He attended elementary school in that city and graduated from Serabul High School in February 1980. In March 1980 he entered Seoul National University, and he received a Bachelor of Science degree in Mining and Petroleum Engineering in February 1984. In the summer of 1984, he entered the University of Tennessee at Knoxville and received a second Bachelor of Science degree in Engineering Science and Mechanics in June 1985.

In September 1985, Mr. Lee started graduate work at the University of Tennessee in Knoxville. He anticipates graduating with a Master of Science degree in Engineering Science and Mechanics in December 1987.